Separation and Purification Technology 353 (2025) 128303

Contents lists available at ScienceDirect

Separation and Purification Technology

journal homepage: www.elsevier.com/locate/seppur

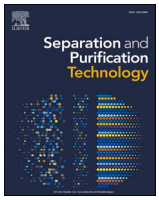

# Recovery of lactose from acid whey by nanofiltration: An experimental study

Marco Roselli, Riccardo Onesti, Cristiana Boi, Serena Bandini *

*Department of Civil, Chemical, Environmental and Materials Engineering – DICAM, Alma Mater Studiorum – University of Bologna, Via Terracini, 28, Bologna I-40131, Italy*

ARTICLE INFO

*Keywords:*
Diafiltration
Membrane characterization
Lactic acid
Electrolytes
Process simulation

ABSTRACT

The flowsheet of an overall process to recover valuable products from raw acid whey is proposed. It considers typical pretreatments, an ultrafiltration step to remove proteins, a decalcification step to remove calcium and magnesium by precipitation, and a nanofiltration/diafiltration step for demineralization and deacidification of lactose. The performance of each step is evaluated and the characteristics of the main streams are estimated. The feasibility of lactose recovery after the decalcification step by nanofiltration is demonstrated by using a spiral wound module. Membrane characterization was performed at pH 4 and 50 °C, with an artificial solution containing lactose, lactic acid and sodium chloride, prepared to mimic the clarified supernatant from the decalcification unit. The feasibility of the simultaneous concentration and deacidification of lactose is finally validated by processing a real solution. With the real solution, the maximum removal of lactic acid, close to 87%, is obtained by operating with a nanofiltration (NF) step (at a concentration factor of 3.5) followed by a NF step operated in diafiltration mode (DF) at constant volume (at a dilution factor of 1.8). A lactic acid/lactose ratio of 0.018 g/g is achieved, with an overall lactose purity and yield of 93.6% and 98.2%, respectively, when operating at low pressure values (up to 12–14 bar). A preliminary process simulation is finally performed to identify the premises for process optimization of the NF+DF configuration. The success of the integrated NF+DF process is contingent upon the correct balance between the choice of the membrane and the operating conditions, which ensure lactose rejections exceeding 98.5% and lactic acid rejections falling below 20–30%, while maintaining transmembrane fluxes between 8 and 15 $dm^3/(hm^2)$.

## 1. Introduction

The recovery of valuable products from whey, typically protein and lactose, is a well-established industry practice for sweet whey and allows a significant reduction in the waste treatment of this by-product [1–5]. However, over the past decade, acid whey has also become a major waste management issue, even though the volume of acid whey produced worldwide is less than that of sweet whey. Acid whey comes from the production of cream and fresh cheeses, such as quark and cottage cheese, and from the production of strained yogurts, such as Skyr and Greek yogurt.

Although the composition of whey is strictly related to the composition of the original milk, acid whey typically has a much lower pH than sweet whey (4.5 vs. 5.8), a lower lactose content (34–43 vs. 44–48 g/$dm^3$), while it has a higher calcium concentration (1–1.6 vs. 0.2–0.5 g/$dm^3$) and a higher lactic acid content (5–9 vs. 0.5–1 g/$dm^3$) than sweet whey; the protein content is about the same [6–10].

While the same valuable elements such as protein and lactose are present in acid whey, very few processes are proposed for their recovery. The higher concentrations of calcium and phosphates and the significantly higher concentration of lactic acid compared to the sweet whey are the main limitations to the processability of acid whey.

At present, most of the published work is devoted to the demineralization and deacidification of raw acid whey with the aim of producing powders that are mainly used for animal feed. The removal of monovalent salts and lactic acid is required to improve the taste of the final product; softening and deacidification are also necessary to allow the processability of the powder. The presence of calcium and lactic acid has negative effects on the crystallization of the lactose contained in the whey, which appears in an amorphous form and produces agglomerates and sticky powders that inhibit spray drying. In addition, calcium and phosphates can interact with proteins and lead to the formation of precipitates in evaporators with significant scaling problems.

* Corresponding author.
*E-mail address:* serena.bandini@unibo.it (S. Bandini).

https://doi.org/10.1016/j.seppur.2024.128303
Received 26 February 2024; Received in revised form 23 May 2024; Accepted 4 June 2024
Available online 13 June 2024

**Nomenclature**

*Abbreviations*

| | |
|---|---|
| LA | lactic acid |
| LT | lactose |

*Symbols*

| | |
|---|---|
| $A_m$ | membrane area ($m^2$) |
| c | concentration ($g/dm^3$) |
| $Jv$, $<Jv>$ | transmembrane flux/average flux (m/s) |
| $L_{p,w}$ | hydraulic permeability ($dm^3/(hm^2bar)$) |
| m | mass (kg) |
| Q | volume flow rate ($m^3/s$) |
| $R_{obs}$ | observed rejection |
| t | generic time |
| V | volume ($m^3$) |
| π | osmotic pressure (bar) |
| Δ | difference |

*Subscripts and superscripts*

| | |
|---|---|
| 0 | at the initial condition |
| *i* | generic solute |
| DF | in diafiltration mode |
| FS | in the feed side (see Fig. 2) |
| NF | in concentration mode |
| P | in the permeate stream (see Fig. 2) |
| PC | in the permeate collector (see Fig. 2) |
| W | water |

Targets for lactose quality can be defined according to the same targets as for lactose from sweet whey: purity greater than 90%, with a maximum lactic acid/lactose ratio of 0.042 g/g. Calcium targets are not well defined. Thorough studies have been carried out recently by various authors [8,11–16], with often contradictory results. The most interesting conclusion reached is the realization that for proper spray dryer operation and good crystallization yield the lactic acid/calcium ratio should be in the range from 1.5 to 2 g/g or in the range from 13 to 14 g/g [14].

Demineralization and deacidification have been proposed by studying the efficiency of conventional techniques such as ion exchange and/or calcium precipitation and membrane processes [6–8,17–24]. Partial demineralization of acid whey is reported in the literature as a consolidated technology [23]: by nanofiltration (NF) of raw acid whey, 40% demineralization was obtained at volume concentration factors of 4, and 70–90% demineralization was achieved by nanofiltration operated in diafiltration (DF) mode at 20 bar [18].

Simultaneous demineralization and lactic acid removal is a more recent subject of study, for which electrodialysis (ED), nanofiltration and/or their integration have been explored. Typically, ED of raw acid whey is effective to achieve 78–90% deacidification and close to 80% electrolyte removal, with remarkably high energy consumption [6,7,22]. The integration of ultrafiltration (UF) with NF (at volume concentration factor of 3.5–4 and 20 bar) was developed by Talebi et al. [8] to remove lactic acid and monovalent electrolytes, but they needed a subsequent ED step to ensure the required softening and deacidification. In their work, the final solution contained 1.6 $g/dm^3$ of calcium and magnesium, it was characterized by a lactic acid/lactose ratio of 0.032 g/g, while ensuring 70% demineralization. Good quality powders were finally obtained by evaporation and drying of a solution obtained by remixing the demineralized and deacidified UF permeate with the UF retentate.

Different strategies to maximize the removal of lactic acid and minerals by avoiding ED have been studied by Chandrapala et al. [19–21]. In [20], they finally proposed the integration of a decalcification step, in which calcium precipitation was favored by the addition of sodium hydroxide, with NF. However, neither NF (at a concentration factor of 3), nor DF (at a volume dilution factor of 3) were effective in the deacidification of microfiltered acid whey: a maximum removal of 66% was obtained at 20 bar, although a 90% removal was claimed to be necessary to meet the purity requirements.

Conversely, very little work has been reported in the literature with the aim of recovering lactose from acid whey [1,25,26]. De Souza et al. [25] report an experimental analysis of several processes and propose, as a best case, the integration of microfiltration with ultrafiltration followed by ion exchange and reverse osmosis to obtain lactose at 95 $g/dm^3$ with 99.8% purity. The effectiveness of lactic acid removal is not mentioned. Kravstov et al. [1] focus on the presence of calcium in acid whey and propose the integration of NF with ED as a possible alternative technique to the decalcification by precipitation. Finally, Casado-Coterillo et al. [26] renew the interest in lactose recovery by performing a preliminary membrane screening on a reconstituted whey, in which lactic acid was artificially added to an ultrafiltered sweet whey. However, the experimental study was only aimed at investigating the role of operative conditions (pH, pressure and temperature) on the lactic acid retention.

All the above-mentioned studies, even if they were mainly addressed to the demineralization and deacidification of whey, give interesting indications and can be used to start research on the recovery of lactose, which could be carried out simultaneously with the recovery of proteins, as is the case of sweet whey. In addition to the removal of monovalent electrolytes, which everyone claims is possible with a NF stage, the studies highlight two aspects that have not yet been resolved. On the one hand, it has not yet been possible to achieve high lactic acid removal rates with NF alone, even after a precipitation decalcification stage. On the other hand, in order to avoid precipitation, softening seems to be possible only by ED, which significantly increases the complexity of the process and could increase the costs of the whole process. Finally, it should not be neglected that in the ED process, the exiting lactic acid together with the bivalent electrolytes represents a waste for the overall process.

The objective of this work is to document the feasibility of demineralization and deacidification of lactose solutions, derived from pretreated acid whey, by NF. Specifically:

a) The overall process flow sheet, which leads from the raw acid whey to the purified lactose, is proposed with the aim of laying the groundwork for the additional recovery of lactic acid.
b) The proof of concept of the step dedicated to the recovery and purification of lactose is first demonstrated through an experimental campaign carried out by testing a NF membrane with an artificial solution, and then validated by testing the same membrane with a real solution.
c) A semi-empirical model is developed to simulate the membrane performances and finally used for a preliminary process analysis.

## 2. The overall process

Fig. 1 shows the flowsheet of the overall process proposed here to recover all the valuable products from raw acid whey. The ultrafiltration (UF) step is the core of the process, where the protein fraction can be separated from the lower molecular weight fraction, containing electrolytes, lactic acid and lactose as main components. UF requires pretreatments such as pasteurization and centrifugation or microfiltration (MF) to inhibit microbial growth and to separate/recover the cream, respectively. UF can be followed by the "lactose recovery and

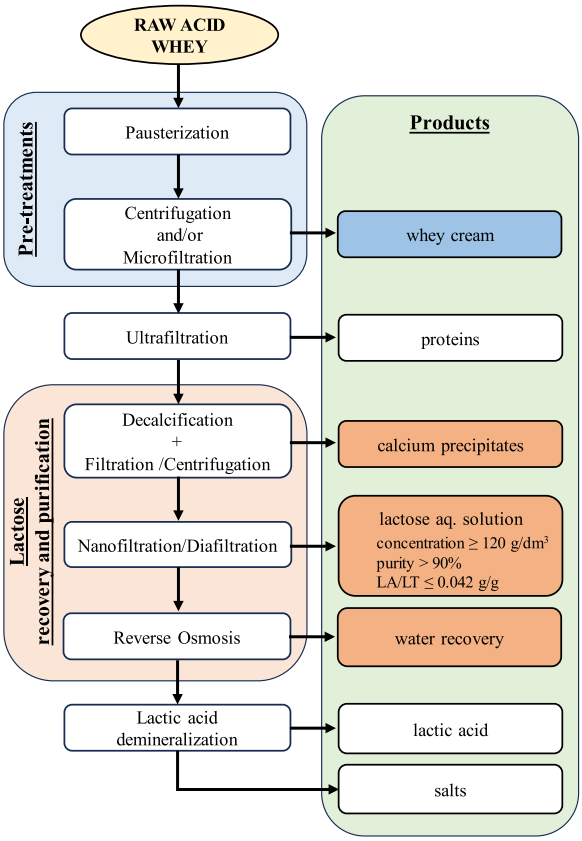


**Fig. 1.** Complete process flowsheet for the recovery of products from acid whey.

purification" step, which requires a decalcification unit and a NF step. If NF is operated in DF mode, a reverse osmosis unit should be considered for water recovery. The chain can be completed with the last step dedicated to "lactic acid demineralization".

For a preliminary feasibility study of lactose recovery and purification in the NF step an experimental investigation was carried out by testing NF membranes with an artificial solution that mimics the supernatant coming from the decalcification step. The characteristics of the artificial solution were determined by prior quantification of the unit operations before the NF step. The operating conditions and the performances of each step were evaluated with reference to the most significant data available in the literature for similar cases; in the absence of information, estimates were based on the consolidated knowledge of each operation.

Details of the quantification of the main items are given below, while specifications of the main streams upstream of the NF unit are summarized in Table 1.

### 2.1. Raw acid whey

The characteristics of raw acid whey can vary depending on the original milk and on the type of cheese being produced. Table 1 shows the average concentration values of the main constituents resulting from the production of cheddar, cottage cheese, Skyr, cream cheese and Greek yogurt as reported in [6,8–10]. In particular, the amounts of lactose and lactic acid are closely related and can vary over a wide range: the higher values of lactic acid (7 g/dm$^3$) correspond to the lower concentrations of lactose (36 g/dm$^3$). The total electrolyte concentration, including phosphates, ranges from 4.1 to 5.4 g/dm$^3$; average values are listed in Table 1.

### 2.2. Pretreatments

The characteristics of the MF permeate (Table 1) are estimated assuming total fat rejection and 5% protein rejection; total permeation of all the other components is considered [4,27].

Pasteurization has no effect on the whey composition.

### 2.3. Ultrafiltration

Useful data for estimating UF efficiency with acid whey can be obtained or deduced from literature information. For proteins, estimates should take into account that protein rejection is affected by the membrane molecular weight cut-off, by the concentration factor achieved and the type of operation (in concentration or DF mode): [7,8,28] report very good rejections, generally higher than 95%. For lactose, [1,7,8,29] report rejection values of UF membranes in the range of 15 to 20%, while [7,8] report rejection values for lactic acid in the range of 5 to 7%. Acid whey mineral rejections are only reported by [7,8]. In summary, the following average rejections were used to estimate the concentrations of the UF permeate stream (Table 1): proteins (95%), lactose (17%), lactic acid (5%), bivalent cations (14%), monovalent cations (−6%), chloride (12%), total phosphates (22%).

### 2.4. Decalcification step

Salt addition at high pH values is proposed to favor the precipitation of calcium phosphates. Clarification of the supernatant by centrifugation and/or MF should be considered to ensure a non-fouling stream to the downstream process. The decalcification efficiency was assessed with reference to the information provided by [20,30]. Ortiz Quezada et al. [30] studied calcium precipitation by addition of tetrasodium pyrophosphate ($Na_2P_2O_7$) while varying the calcium to phosphorus ratio (Ca/P), pH values, temperature and holding time. Several effective combinations were proposed, but for the purposes of this work, the operating conditions of the decalcification step were selected to ensure the highest calcium removal. At pH 10 (obtained by adding a NaOH solution), Ca/P ratio of 0.8 mol/mol (obtained by adding tetrasodium pyrophosphate), 55 °C and a holding time of 35 min, Ortiz Quezada et al.

**Table 1**
Characteristics of a typical raw acid whey, main streams before NF step and artificial solution.

| | Units | Raw acid whey | MF Permeate | UF permeate | Decalcification supernatant (after clarification) | NF feed (artificial solution) |
|---|---|---|---|---|---|---|
| lactose (LT) | g/dm$^3$ | 36–43 | 36–43 | 29–37 | 26–33 | 30 |
| lactic Acid (LA) | g/dm$^3$ | 7–5.4 | 7–5.4 | 6.7–5.0 | 5.3–3.9 | 4.4 |
| fats | g/dm$^3$ | 0.10 | – | – | – | – |
| proteins | g/dm$^3$ | 3.0–4.5 | 2.8–4.3 | 0.14–0.22 | – | – |
| Ca + Mg | g/dm$^3$ | 1.35 | 1.35 | 1.16 | 0.02 | – |
| Na + K | g/dm$^3$ | 1.70 | 1.70 | 1.81 | 1.81 | 1.6 |
| Cl | g/dm$^3$ | 1.01 | 1.01 | 0.88 | 0.88 | 1.2 |
| P | g/dm$^3$ | 0.70 | 0.70 | 0.55 | 0.55 | – |
| pH | – | 4.6 | 4.6 | 4.6 | 10 | 4 |
| LA/LT | g/g | 0.19–0.13 | 0.19–0.13 | 0.23–0.14 | 0.20–0.12 | 0.15 |

[30] reported a calcium removal of 98%, while the residual concentration of phosphates was been estimated to be 0.55 g/dm$^3$. The final concentrations of the clarified supernatant from the decalcification step, as reported in Table 1, were estimated by assuming 21% lactic acid removal and 9% lactose loss (as measured by [20]); a total removal of proteins was considered (as a consequence of their complexation with calcium and precipitation), while negligible effects on electrolyte removal were assumed.

### 2.5. Nanofiltration

The quantification of the NF step is the main subject of the next sections, where an experimental study is presented to show the membrane performances and the process efficiency in demineralization and deacidification.

The study described here ends with the characterization of the NF step, while the efficiency of the "lactic acid demineralization" step (Fig. 1) is not evaluated. For this purpose, it is currently possible to refer to the operations typically used for the recovery and purification of lactic acid downstream of the bioreactors [31,32], taking into account the better quality of the lactic acid solution generated by the process proposed here.

The main objectives of the NF unit are: i) to ensure the removal of lactic acid to obtain a lactic acid/lactose ratio lower than 0.042 g/g; ii) to obtain a demineralization of at least 70%, with a total lactose purity higher than 90%; iii) to reach the lactose concentration of 120 g/dm$^3$, which is usually accepted as economically convenient for the subsequent evaporation prior to crystallization.

## 3. Materials and methods

### 3.1. Materials

#### 3.1.1. Solutions

The artificial solution (Table 1) was prepared by dissolving lactose (342 kg/kmol), sodium chloride (58.4 kg/kmol) and lactic acid (90.1 kg/kmol, pKa=3.90 at 50 °C [33]) in demineralized water (5.0 μS/cm, pH 4.7). Reagent grade alpha-monohydrate lactose (Carlo Erba Reagents s.r.l.-Milan, Italy), sodium chloride (Merck SpA-Milan, Italy) and lactic acid (Fisher Scientific Italia-Milan, Italy), that was available in aqueous solution at 85–90% w/w, were used; pH was adjusted by adding NaOH.

The real solution (Table 2) was prepared by dissolving the powder of ultrafiltered sweet whey (Reire srl, Reggio Emilia-Italy) in demineralized water with the addition of lactic acid (at 85–90% w/w), obtaining a solution with a composition very similar to that of the stream coming from the decalcification unit, in terms of lactose, lactic acid and total electrolytes. The composition of the reconstituted real solution is particularly conservative with respect to the artificial solution; in fact, the presence of proteins and a modest amount of fats could reduce membrane performance compared to the case of the artificial solution. Finally, for the purposes of determining the lactic acid/lactose ratio and demineralization, the presence of calcium can be considered irrelevant, while the presence of phosphates and sulfates renders the real solution more representative of the decalcification supernatant (Table 1).

**Table 2**
Characteristics of the real solution.

| Solute | Concentration (g/dm$^3$) | Electrolyte | Concentration (g/dm$^3$) |
|---|---|---|---|
| Proteins* | 0.88 | Sodium + potassium | 0.62 |
| Fats* | 0.07 | Chloride | 0.23 |
| Lactose | 29.6 | Calcium + magnesium | 0.30 |
| Lactic acid | 4.33 | Phosphates | 0.74 |
| Total electrolytes | 2.6 | Sulphates | 0.07 |

(*) = calculated from the technical data sheet of the sweet whey powder.

#### 3.1.2. Membrane

All the NF experiments were performed with a DK1812 spiral wound module (0.38 m$^2$ nominal membrane area, 34 mil feed spacer, 12″ module length and 1.85″ diameter) manufactured by Veolia Water Technologies SpA., which supports DK membranes. DK membranes are thin film composite NF membranes with a polyamide active layer supported on polysulfone, 150–300 Da MWCO and 98% $MgSO_4$ nominal rejection measured with 2000 ppm $MgSO_4$ solutions at 25 °C and 7.6 bar [34].

The selection of the DK membrane was guided by the synthesis of several literature results, as referenced in [35–40]. Typically, the DK membrane shows high disaccharide rejections even at 50 °C, in comparison to other similar membranes such as DL. Additionally, it exhibits lower rejections for monovalent electrolytes in comparison to other similar membranes, as evidenced by the NF270 membranes-FilmTec$^{TM}$, which operate at low pressures (5–10 bar) and pH 4, which is very close to the point of zero charge of the membrane. On the other hand, in [19,21], the authors screened membranes (DK, DL, HL, by Veolia, and XN45-Trisep) with real acid whey at 21 bar, selecting the HL. However, the DK was found to have a higher lactose rejection, albeit lower fluxes. Subsequent results [20], demonstrated that the HL membrane was unable to achieve the required lactic acid removal. Consequently, the DK membrane was selected for this study as the optimal compromise between the need for high lactose rejection and the need for high transmittance of lactic acid and electrolytes.

#### 3.1.3. Equipment

All the experiments were performed in a bench-scale NF apparatus [35], modified to operate in both concentration mode and DF mode at constant volume. The detailed flowsheet is reported in the supplementary material with a photo of the apparatus (Figures S1 and S2), simplified schemes are reported in Fig. 2 for clarity.

Fig. 2a) refers to NF operating in concentration mode: the feed tank is initially filled with the artificial solution, the retentate is continuously

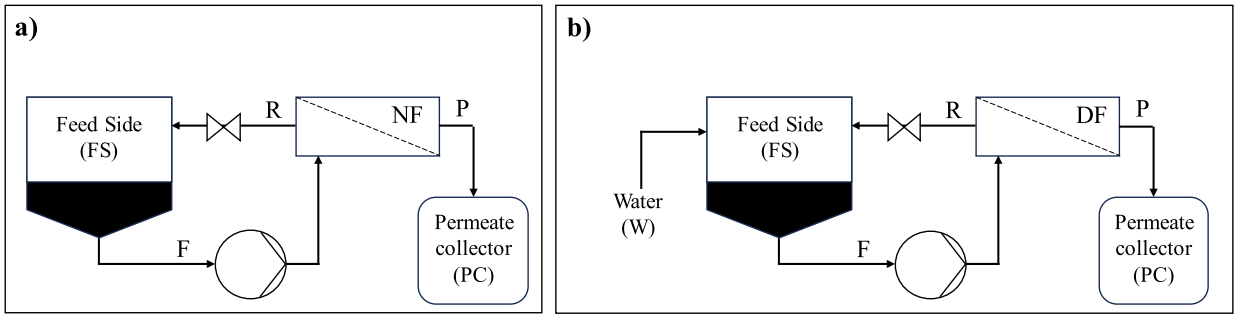


**Fig. 2.** Diagram of the experimental apparatus operating a) in concentration mode, and b) at constant volume DF mode.

recirculated to the tank while the permeate is continuously collected downstream of the module. During a NF experiment, the volume of the feed side decreases with time while the total concentration increases. At any time, the parameter *VCF*, the Volume Concentration Factor, can be defined accordingly as the ratio of the initial volume of the solution in the feed side to the volume of the solution in the feed side at the corresponding time.

Fig. 2b) shows the scheme of the NF operating with constant volume DF mode: demineralized water (maintained at pH 4, by adding an HCl solution) is continuously added to the feed tank to keep the volume constant over time, i.e. the water volumetric flow rate is kept equal to the permeate flow rate, which in turn can vary over time. A dosing pump is used for this purpose. At any time, the parameter *VDF*, Volume Dilution Factor, can be defined accordingly as the ratio of the volume of the permeate collected (corresponding to the volume of water added) to the initial volume of solution in the feed side. In all the experiments, the pH was measured in the feed side and in the permeate collector.

With the same apparatus, the integration of NF with DF (NF+DF) was also studied, where the final retentate of the previous concentration step was used as initial feed for DF.

### 3.2. Experimental and analytical methods

According to the standard protocol already presented and discussed in [35,41], the virgin module was stabilized with demineralized water at 10 bar and 50 °C; after each experiment, the module was rinsed with demineralized warm water (at 40 °C) and subjected to an acid-base washing, at pH 4 and 10, respectively. The effectiveness of the rinsing/washing procedure was checked by comparing the hydraulic permeability with the value measured with the stabilized module. An average hydraulic permeability of 10.17 ± 0.73 $dm^3/(hm^2bar)$ was obtained during the whole campaign, in excellent agreement with the values measured with other samples of the same type of membranes [41]. A rinsing/washing procedure was performed after each experiment in order to test the membrane under the same conditions and obtain comparable data with a clean membrane.

All the experiments were performed at 50 °C, pH 4 and 600 $dm^3/h$ feed flow rate, corresponding to a superficial velocity of 0.36 m/s [41].

The temperature of 50 °C was chosen to obtain high transmembrane fluxes and to limit microbial growth, although the preservative properties of lactic acid are favorable per se.

The feed flow rate was selected to control polarization phenomena which may be present due to the high lactose concentrations. The experiments did not reveal any significant permanent fouling, likely due to the favorable combination of low transmembrane fluxes and a very high superficial velocity.

The pH value of 4 was chosen as a good compromise between the need to achieve the highest lactate permeation, the need to limit corrosion problems and the need to avoid the use of expensive equipment materials. It is well-known that the rejection of organic acids decreases with decreasing pH, and that the highest permeation in a NF membrane occurs at pH values lower than 5, corresponding to the lowest dissociation degrees of the acids [19,20,26,36,42,43]. Furthermore, as the pH value of 4 corresponds to the isoelectric point of the membrane, the minimum rejection of monovalent electrolytes can be anticipated, which is highly favorable for demineralization.

Experiments in concentration mode were carried out to obtain *VCF* values ranging from 2 to 3.8. The experiments with the artificial solution were performed at constant transmembrane pressure (TMP) (at 11.6, 15.6 and 19.6 bar) and at constant average permeate flux (STEP mode). The STEP mode was performed by increasing the pressure by 2 bar per step to ensure average permeate fluxes in the range of 6.5 to 9.5 $dm^3/(hm^2)$ as the concentration increased with time. Such an approach was adopted to favor lactose rejection and to promote the simultaneous removal of lactic acid and electrolytes. In fact, scientific evidence shows that the rejection of low molecular weight solutes decreases significantly as the permeate flux decreases, while the rejection of higher molecular weight neutral solutes is affected to a lesser extent [44,45]. The experiments with the real solutions were performed in accordance with the STEP-mode.

DF experiments with the artificial solution as it is were performed to achieve *VDF* values close to 2.4, by operating at TMP values of 3.7 bar corresponding to the minimum TMP that could be regulated in the experimental apparatus. In these conditions, average permeate fluxes in the range of 9–9.5 $dm^3/(hm^2)$ were obtained.

The DF experiments, integrated with a NF in concentration mode, were performed at TMP values to ensure average permeate fluxes close to 9 $dm^3/(hm^2)$, both with the artificial solution and with the real solution.

For each experiment, permeate flux was measured at regular intervals and samples of the feed tank, permeate stream and permeate collector were taken and analyzed.

Lactose and lactic acid concentrations were measured by HPLC, using a Prominence Modular HPLC from Shimadzu Italia s.r.l. (Milan, Italy), equipped with an ORH801 organic acid column (Sepachrom s.r.l., Milan, Italy) and a refractive index detector. Analyses were performed using 0.1 N $H_2SO_4$ as the mobile phase, at a flow rate of 0.5 mL/min and at a temperature of 35 °C for both the column and the detector.

Cation and anion concentrations were measured using two Dionex™ Aquion™ Ion Chromatography Systems from Thermo Fisher Scientific (Milan, Italy). A Dionex™ IonPac™ CS12A IC column equipped with a Dionex™ CDRS 600 suppressor was used to measure the cations. Analyses were performed using 4.5 mM sodium carbonate / 0.8 mM sodium bicarbonate as eluent, at a flow rate of 1 mL/min and a column and detector temperature of 30 °C and 35 °C, respectively.

A Dionex™ Integrion™ HPIC system, equipped with a Dionex™ AERS 500 suppressor, was used for anions measurements. Analyses were performed using methanesulfonic acid as the eluent, at a flow rate of 1 mL/min and a column and detector temperature of 40 °C and 35 °C, respectively.

Given the total rejection of the membrane by proteins and fats, the concentrations of these substances in the real solution were calculated in accordance with the obtained VCF.

### 3.3. Characterization parameters

The definition of the parameters used along the paper is reported here. A summary of the overall notation is listed in the Nomenclature.

The separation efficiencies of the NF, DF and NF+DF operations are defined in (1)-(3), in which the notations of Fig. 2 are mentioned.

$$\text{lactic acid/lactose ratio} = \frac{LA\ concentration\ in\ the\ feed\ side}{LT\ concentration\ in\ the\ feed\ side} \tag{1}$$

$$\text{lactose purity} = \frac{LT\ concentration}{LT + LA + electrolytes\ concentration} \tag{2}$$

$$\text{demineralization} = \frac{mass\ of\ electrolytes\ in\ the\ permeate\ collector}{initial\ mass\ of\ electrolytes\ in\ the\ feed\ side} \tag{3}$$

For the real solution, lactose purity was calculated taking into account the concentration of all substances present, including proteins and fats.

In order to characterize the membrane, the typical quantities of total transmembrane flux ($flux = \frac{Q_P}{A_m}$) and the observed rejection of $i$ solute ($rejection = 1 - \frac{c_i^P(t)}{c_i^{FS}(t)}$) were measured as a function of time.

In addition, at each time $t$, the following parameters are calculated according to Eqs. (4)-(7), which are obtained by combining the total mass balance and the $i$ solute mass balance equations applied to the corresponding experimental system (Fig. 2).

For the NF in concentration mode (NF), *VCF* and the removal of the *i-th* solute (REMOVAL) can be calculated as follows:

$$VCF(t) = \frac{V_0^{FS}}{V^{FS}(t)} = \frac{c_i^{FS}(t) - c_i^{PC}(t)}{c_{i,0}^{FS} - c_i^{PC}(t)} \quad (4)$$

$$REMOVAL_i(t) = \frac{VCF(t) \times c_{i,0}^{FS} - c_i^{FS}(t)}{VCF(t) \times c_{i,0}^{FS}} \quad (5)$$

For the NF in diafiltration mode (DF) at constant volume, *VDF* and the removal of the *i-th* solute can be calculated as follows:

$$VDF(t) = \frac{V^{PC}(t)}{V_0^{FS}} = \frac{c_{i,0}^{FS} - c_i^{FS}(t)}{c_i^{PC}(t)} \quad (6)$$

$$REMOVAL_i(t) = \frac{c_{i,0}^{FS} - c_i^{FS}(t)}{c_{i,0}^{FS}} \quad (7)$$

In Eqs. (4)–(7), $c_{i,0}^{FS}$ represents the initial solute concentration in the feed side, and $c_i^{PC}$ is the solute concentration in the permeate collector; lactose concentration was used to evaluate *VCF*, while lactic acid concentration was used to calculate *VDF*.

Finally, the overall removal of the *i-th* solute in the integrated NF + DF configuration is calculated according to Eq. (8).

$$OVERALL\ REMOVAL_i(t) = \frac{VCF_{NF} \times c_{i,0}^{FS,NF} - c_i^{FS,DF}(t)}{VCF_{NF} \times c_{i,0}^{FS,NF}} \quad (8)$$

where $VCF_{NF}$ represents the overall *VCF* achieved in the NF step.

It can be observed that the corresponding definitions of removal also be used to quantify the lactose loss in the permeate collector as well as the percent demineralization, as reported in the results. In addition, the removal of lactic acid corresponds to the yield of separation, whereas the yield of lactose recovery can be obtained as (1-REMOVAL).

## 4. Experimental results

### 4.1. Membrane characterization

The membrane performances measured in the NF experiments (in concentration mode) with the artificial solution (Table 1) are summarized in Fig. 3 and 4. Fig. 3 shows the evolution of the total transmembrane flux; the data are reported along the VCF in the constant TMP experiments (Fig. 3a) and along the lactose concentration in the feed side in the STEP-mode experiments.

Apparently, the typical behavior of decreasing flux with increasing concentration at a constant TMP value is observed in Fig. 3. This is due to the increasing effect of the osmotic pressure of lactose, which is the most retained solute. Operating at high TMP values allows higher fluxes to be obtained and correspondingly higher *VCF* could be achieved.

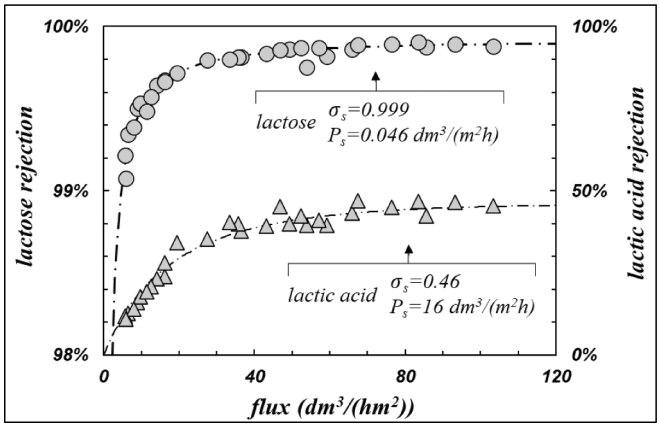


**Fig. 4.** Observed rejections of lactose and lactic acid versus total transmembrane flux in NF concentration mode of the artificial solution. Dashed lines are the predictions obtained by the 3-parameter model (Eq. (9)) using the corresponding reflection coefficients and solute permeabilities.

Fig. 3a) evidences that the TMP of 11.6 bar can be considered as the minimum operating pressure to achieve a *VCF* of 3.55, which corresponds to a lactose concentration of 111 g/dm$^3$. Comparing the results of Fig. 3a) with the data of Fig. 3b), it can be observed that the operating mode does not affect the achievable lactose concentration: a lactose concentration of 113 g/dm$^3$ was also obtained in STEP-mode, at the corresponding TMP of 11.7 bar. However, the STEP-mode operation allows to keep the total fluxes in the range from 4 to 16 dm$^3$/(hm$^2$), with average values contained in the range from 6.5 to 9.5 dm$^3$/(hm$^2$), with interesting advantages regarding the rejection values.

Fig. 4 collects all the observed rejections of lactose and lactic acid as a function of total flux, obtained in the experiments in concentration mode at constant TMP and in STEP-mode. As expected from literature data with similar membranes and similar compounds, lactose rejection is very high, greater than 99 % even at very low fluxes, and is independent of lactose concentration, as is typical for neutral compounds [26,35,46].

Lactic acid rejection, on the other hand, varies over a wider range: it increases steadily from 10% to 35% in the flux range from 5 to 20 dm$^3$/(hm$^2$) and approaches an asymptotic rejection close to 45% at 70 dm$^3$/(hm$^2$). However, it is important to note that, in the range of concentrations studied, the lactic acid rejection vs. flux curve is not affected by the lactic acid concentration (varying in the range from 4.47 to 8 g/dm$^3$), nor by the lactose concentration (varying in the range from 30 to 113 g/dm$^3$). Furthermore, it can be observed that no effect of the electrolyte concentration could be detected on lactic acid rejection, as the

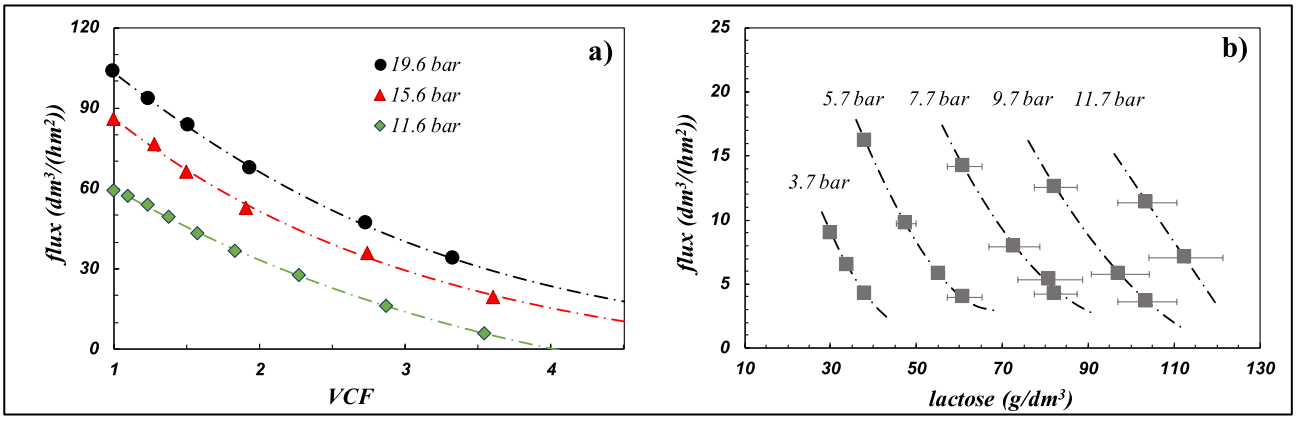


**Fig. 3.** Variation of the permeate flux in NF experiments (concentration mode) with the artificial solution at a) constant TMP and b) in STEP-mode. Pressure values are the corresponding TMP. Dashed lines are the fitting curves.

NaCl concentration remained rather constant at 2.8–2.9 g/dm$^3$. This is due to the very low NaCl rejection, mainly favored by low fluxes and by the operating pH close to the isoelectric point of the DK membrane.

These behaviors are remarkably interesting: operating the NF at low fluxes should facilitate greater permeation of lactic acid with correspondingly minimal lactose loss in the permeate. At low fluxes, i.e. low TMPs, lactic acid rejection decreases to a greater extent than lactose rejection. For instance, at a flux of 10 dm$^3$/(hm$^2$), lactic acid rejection is approximately 18%, while lactose rejection is about 99.5%. When the flux is increased to 30 dm$^3$/(hm$^2$), lactic acid rejection increases to 38%, while lactose rejection is approximately 99.8%. In the most unfavorable scenario, which is working under asymptotic conditions, the lactic acid rejection would be increased to 46% against a lactose rejection of 99.9%. It is evident that the optimal operating conditions for achieving the most effective separation between lactose and lactic acid are at fluxes that do not exceed 30 dm$^3$/(hm$^2$). The results reported in the next section will document this evidence.

Finally, it can be noted that the obtained behaviors can be described according to a common 3-parameters semi-empirical model, such as the well-known Spiegler-Kedem or Mason-Lonsdale models [47]. The reflection coefficients ($\sigma_s$) and the solute permeabilities ($P_s$) of lactose and lactic acid are calculated by fitting the experimental data with the relationships given in Eq. (9):

$$rejection = \frac{(e^{Pe}-1)\sigma_s}{e^{Pe}-\sigma_s} \quad \text{with} \quad Pe = \frac{(1-\sigma_s)J_v}{P_s},\ \lim_{J_v\to\infty}(rejection) = \sigma_s \tag{9}$$

where the correspondence of ($\sigma_s$) with the asymptotic rejection is recalled. The parameter values are reported in Fig. 4. The curves predicted with Eq. (9) (lines) document the good quality of the fitting.

### 4.2. Nanofiltration in concentration mode

The most representative results obtained in the NF experiments (concentration mode) with the artificial solution are summarized in Fig. 5.

The ability of the DK membrane to remove lactic acid from the artificial solution is well documented in Fig. 5a) and b), where the effect of the pressure mode is clearly demonstrated. As would be expected from the results of Fig. 4, operating at average fluxes in the range from 6.5 to 9.5 dm$^3$/(hm$^2$), as provided by the STEP-mode, is much more effective in removing lactic acid. In fact, with an initial lactic acid concentration of 4.6 g/dm$^3$, when operating at constant TMP values in the range from 11.6 to 19.6 bar, at *VCF*=3.5 the lactic acid removal is lower than 55.6%, whereas in the STEP-mode the removal is 64.4%. Correspondingly, the lactic acid concentration in the feed residue increases up to 8.1 g/dm$^3$ at 19.6 bar, with fluxes ranging from 100 to 30 dm$^3$/(hm$^2$), while it is limited to 5.5 g/dm$^3$ in the STEP-mode. Conversely, operation in STEP-mode leads to a higher lactose loss in the permeate, but well below 1% (Fig. 5d). This trend appears to be consistent with the lactose rejection data (Fig. 4), which show a slight decrease of lactose rejection at low fluxes.

The most interesting results are shown in Fig. 5c), where the LA/LT ratio is plotted against *VCF*. Apparently, none of the pressure operation modes is able to reach the target value of 0.042 g/g, at *VCF* values close

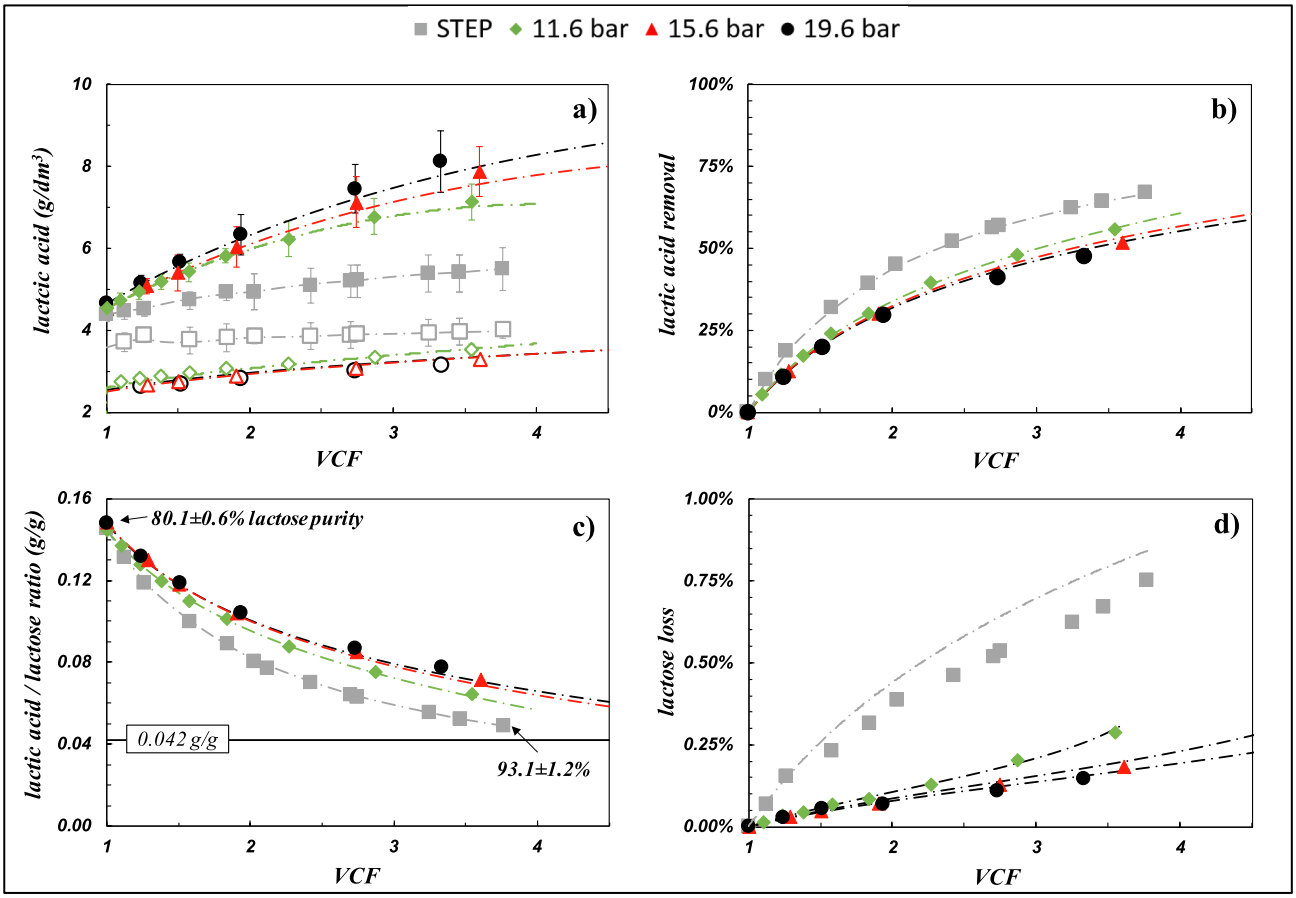


**Fig. 5.** Effect of pressure operation mode on NF (concentration mode) performance with the artificial solution. a) Lactic acid concentration in the feed side (closed symbols) and in the permeate collector (open symbols); b) Lactic acid removal; c) LA/LT ratio in the feed; d) Lactose loss in the permeate collector. Dashed lines are the corresponding simulations by the semi-empirical model (Table 3).

to 4, although the STEP-mode is the most effective. Increasing the pressure in STEP-mode above 11.6 bar would have been unfavorable, since it would have increased the lactic acid rejection and, most likely, the asymptotic removal would have been approached. The STEP-mode is also effective for demineralization: a lactose purity of 93% is achieved at a *VCF* close to 3.8, with a demineralization of 73%.

Finally, it can be noted that the pressure operation mode does not significantly affect the lactose concentration in the retentate as a function of *VCF*, since the lactose rejections are higher than 99%. As documented in Fig. S3 of the Supplementary Information, the concentration of 110 g/dm$^3$ was obtained in the different experiments with the artificial solution.

Fig. S3 also shows a comparison between the pH measured in the permeate collector and the corresponding values in the feed side. The pH changes in the feed side are very small, between 4 and 4.1. The pH of the permeate is always lower than that of the feed side, but between 3.9 and 4.05, indicating negative proton rejection, in agreement with other results obtained with these membranes [48].

### 4.3. Nanofiltration in diafiltration mode

The main results obtained in the DF experiments with the artificial solution as it is (Table 1) are summarized in Fig. 6. DF is very effective in removing lactic acid: the concentration in the feed side is halved by increasing the *VDF* from zero to 0.8, and the value of 0.72 g/dm$^3$ can be obtained at a *VDF* of 2.4. Also in this case, the experiments were carried out at a very low TMP (3.7 bar) in order to ensure low values of the average flux, which varied between 8 and 10.5 dm$^3$/(hm$^2$); accordingly, the lactose concentration remained rather constant (30 g/dm$^3$) during the experiments.

This behavior confirms the high rejections observed for lactose with the DK membrane, which are even more favored by the low lactose concentration. Details of the evolution of the lactose concentration in the feed side and the total flux along the *VDF* are shown in Fig. S4 of the Supplementary Information, where a comparison between the pH measured in the permeate collector and the corresponding values in the feed side is also reported. Also for DF, the pH changes in the feed side are very small (from 4.05 to 4.18); however, it should be noted that DF is performed with demineralized water at pH 4. Again, the pH of the permeate is always lower than that of the feed, confirming the negative proton rejection.

It is remarkably shown in Fig. 6b) that the DF mode allows to reach the target of LA/LT=0.042 g/g at VDF=1.7. Higher lactose purities can be obtained by operating at *VDF*=2.4, which leads to a LA/LT ratio close to 0.024 g/g, with a demineralization of 89%, corresponding to a lactose purity of 96.7%.

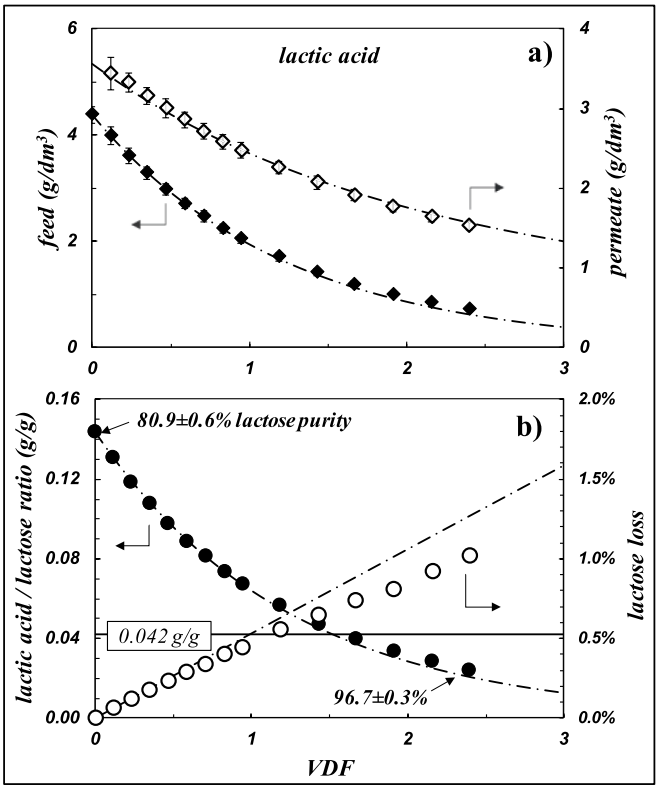


**Fig. 6.** NF performance in DF mode at TMP=3.7 bar with the artificial solution. a) Lactic acid concentration in the feed (closed symbols) and in the permeate collector (open symbols); b) LA/LT ratio in the feed and lactose loss in the permeate collector. Dashed lines are the corresponding simulations by the semi-empirical model (Table 3), at average flux=9.4 dm$^3$/(hm$^2$).

### 4.4. Discussion: The integrated NF+DF process

Although operation in DF mode of the artificial solution as it is leads to high quality lactose, it requires large amounts of water, the recovery of which should be considered as an additional step. However, in order to recover all the water needed for the DF operation and to concentrate the DF retentate to achieve a concentrated purified lactose, two additional reverse osmosis steps should be envisaged: one dedicated to the concentration of the residual feed and another dedicated to the concentration of the permeate from the DF step.

A good compromise can be represented by the integration of a NF step (operated in concentration mode) with a subsequent DF step (operated at constant volume).

The experimental evidence reported in the previous sections suggested performing both operations while keeping the total flux values constant. Specifically, the NF of the artificial solution was carried out up to *VCF*=2.12 with an average flux of 8.5 dm$^3$/(hm$^2$), regulating the pressure according to a STEP-mode in the range from 3.7 to 6.7 bar; the DF was carried out up to *VDF*=2.0 with an average flux of 8.8 dm$^3$/(hm$^2$), at TMP=6.7 bar. The main results are shown in Fig. 7. The concentration step (NF) allows to remove a significant part of lactic acid (47.3%) with a simultaneous concentration of lactose (64.1 g/dm$^3$). Accordingly, a lactose loss of 0.4% was measured in the permeate, with an electrolyte removal of 47.5%, giving a solution with a lactose purity of 89.1%.

The subsequent DF step effectively completes the deacidification and demineralization. At *VDF*=1, the LA/LT ratio can be remarkably reduced to 0.034 g/g, corresponding to a lactic acid removal of 77.7% and a demineralization of 83.1%, ensuring an overall lactose purity of 95.3%. Fig. 7, on the other hand, documents the possibility of obtaining 89% lactic acid removal at VDF=2.0, with a corresponding LA/LT ratio of 0.014 g/g and an overall lactose purity of 97.8%.

All the results obtained so far in this work provide experimental evidence that the lactic acid removal required to ensure good quality lactose can be obtained by operating in the NF+DF mode, at least with an artificial solution, by maintaining appropriate operating conditions. The lactic acid removal achieved in this work was much higher than the 66% value recognized as the maximum achievable by Chandrapala et al. [20]. In [20] the authors worked with the HL membrane, under favorable conditions of VDF=3 and pH 3, but in the presence of high amounts of proteins, since they did not consider an UF step prior to NF, which was strongly affected by remarkable fouling.

The results of this work are also consistent with those obtained by Talebi et al. [8] in the case of acid whey demineralization. They achieved LA/LT=0.032 g/g by integrating NF (at VCF=3.5–4 and TMP=20 bar) with ED, treating the UF permeate at the natural pH of acid whey, whereas the integration of NF (at VCF=3.5–4) with DF (at VDF=1 and TMP=20 bar) led to a value of LA/LT of only 0.040 g/g.

In this respect, it is very interesting to note that, to the best of our knowledge, none of the authors [6,8,19,21] who have worked with acid

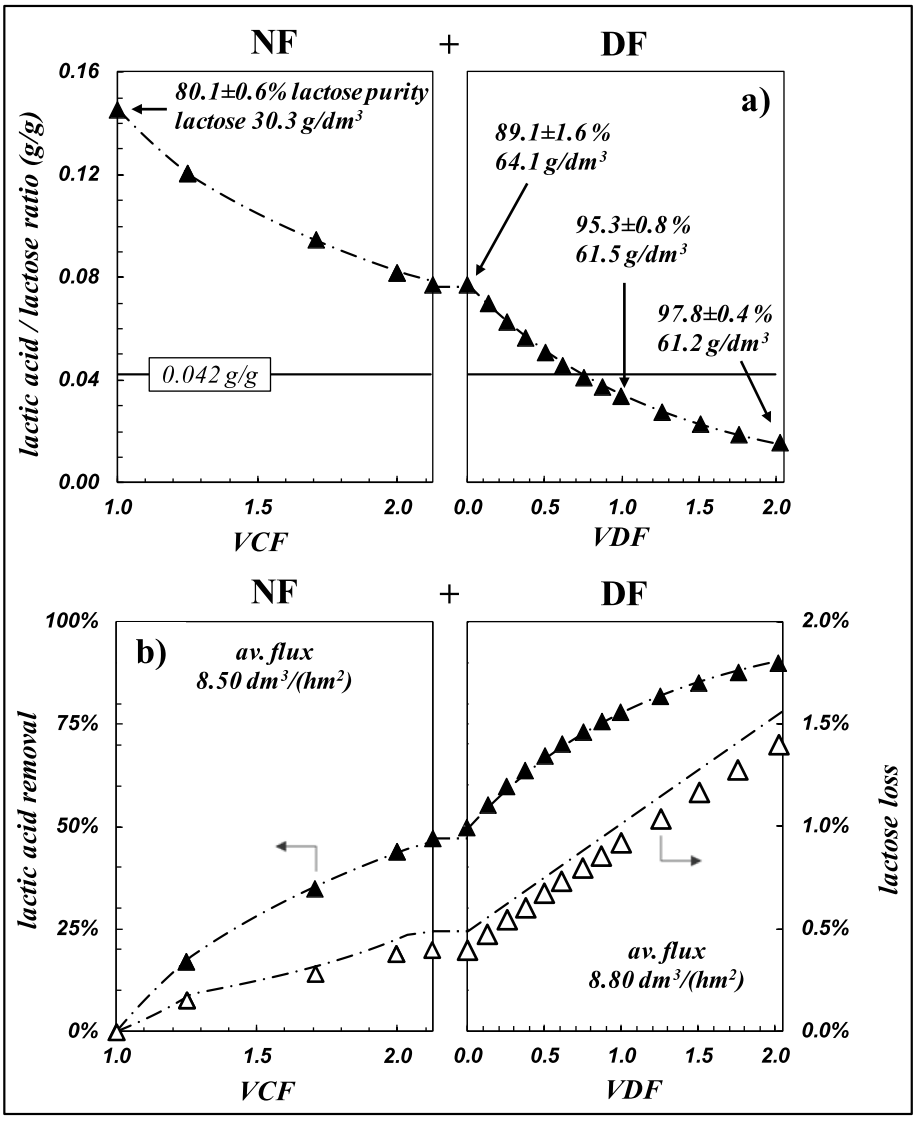


**Fig. 7.** Performance of the integrated NF+DF process with the artificial solution. NF is operated in STEP-mode (3.7–6.7 bar), DF is operated at TMP=6.7 bar. a) LA/LT ratio in the feed; b) lactic acid removal and lactose loss in the permeate collector. Lactose purity and feed side concentration are shown for the corresponding conditions. Dashed lines are the corresponding simulations by the semi-empirical model (Table 3), at the corresponding average fluxes.

whey report information on lactose loss, either in the NF or in the ED stage. Only Cuartas-Uribe et al. [46], with the aim of demineralizing lactose from sweet whey, report as acceptable a total lactose loss of 10% by operating a NF (VCF=2) followed by a DF (VDF=2) with DL membranes (slightly more permeable and less selective than DK) at 20 bar. The case is roughly homologous to that shown in Fig. 7, where instead lactose losses of no more than 1.5% are obtained.

As documented in this work, operating at low transmembrane flux, by keeping TMP values lower than 20 bar, both in NF and in DF mode, opens the possibility of avoiding the ED step, with the advantages related to the use of a unique process that could be carried out with the same membrane and therefore with the same equipment. In addition, operating at low pressures should reduce energy consumption and, at the same time, increase the required membrane area.

However, the experiments documented in Fig. 7 refer to the case where the purified lactose is obtained at a relatively low concentration (close to 60 g/dm$^3$), corresponding to a VCF=2.

The experimental evidence of the feasibility of the simultaneous lactose concentration and purification obtained by processing the real solution (Table 2) is shown in Fig. 8, where the results are reported in the case of the integration of NF with DF.

Specifically, the NF was performed up to *VCF*=3.52 with an average flux of 8.6 dm$^3$/(hm$^2$), regulating the pressure according to a STEP-mode in the range from 4.6 to 11.6 bar; the DF was carried out up to *VDF*=1.81 with an average flux of 9.0 dm$^3$/(hm$^2$), at TMP=13.5 bar. A significant and interesting confirmation of the trends and results obtained in the case of the artificial solution can be observed. The concentration step (NF) allows the removal of 60.3% of lactic acid with a simultaneous concentration of lactose up to 103.5 g/dm$^3$, resulting in an overall lactose purity of 88.5%; as in the case of the artificial solution, the loss of lactose in the permeate is relatively low (0.65%). The subsequent DF step effectively completes the deacidification. At *VDF*=0.92, the LA/LT ratio can be remarkably reduced to 0.030 g/g, corresponding to a lactic acid removal of 79.7%, ensuring an overall lactose purity of 92%. The lactic acid concentration varied from 4.33 to 6.05 in the NF step, while in the DF step it decreased to 1.89 g/dm$^3$. However, experiments document the possibility of achieving 87.6% lactic acid removal at VDF=1.81, with a corresponding LA/LT ratio of 0.018 g/g and an overall lactose purity and lactose loss in the permeate of 93.6% and 1.81%, respectively.

Overall, the results obtained with the artificial solution (Fig. 7) and those obtained with the real solution (Fig. 8) clearly show that it is

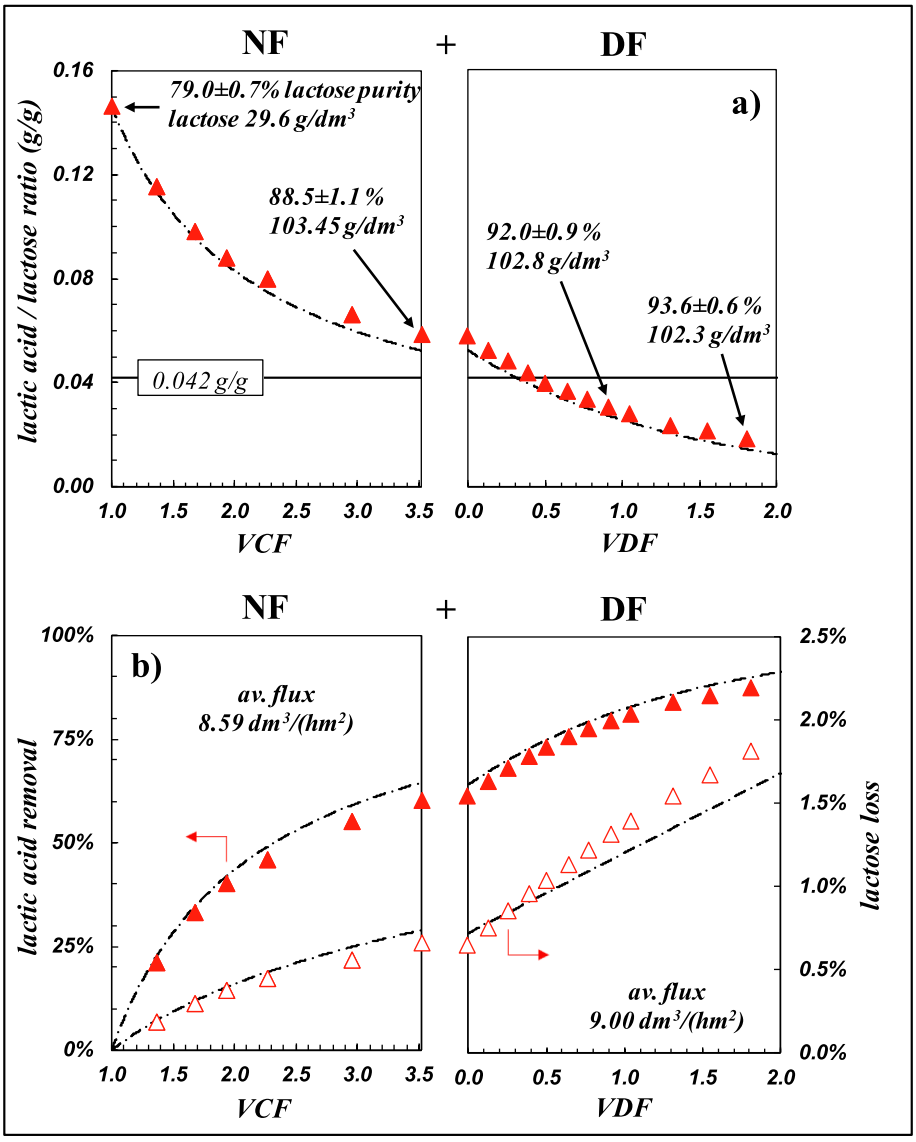


**Fig. 8.** Performance of the integrated NF+DF process with the real solution. NF is operated in STEP-mode (4.6–11.6 bar), DF is operated at TMP=13.5 bar. a) LA/LT ratio in the feed; b) lactic acid removal and lactose loss in the permeate collector. Lactose purity and feed side concentration are shown for the corresponding conditions. Dashed lines are the corresponding simulations by the semi-empirical model (Table 3), at the corresponding average fluxes.

possible to achieve the specifications of deacidification (LA/LT < 0.042 g/g) and lactose purity (>90%) given as a primary objective to obtain lactose of the quality required by the industry, at least operating with average fluxes in the range of 8–9 $dm^3/(hm^2)$ in the NF stage. Finally, a cross comparison between the results obtained with the artificial solution (Figs. 5 and 7) and those obtained with the real solution (Fig. 8) shows that the artificial solution is indeed a good simulation of a real solution.

At this point of the study, it becomes interesting to understand which, if any, are the best NF + DF combinations to obtain higher lactose concentrations with the required level of deacidification. The simulations presented in the next section allow to draw interesting conclusions.

## 5. Modeling and simulations

In this section, a semi-empirical model is presented to simulate the performance of NF and DF processes. First, the cases studied in the previous experiments are considered. Then, additional simulations are reported for a final discussion.

The processes depicted in Fig. 2 can be described by the equations given in Table 3, where the mass balance equations are written under the constant density hypothesis.

When simulating NF in the concentration mode, Eqs. (10)-(11) can be integrated along time by using the appropriate boundary conditions. The integration was performed according to Euler's method [49], simply implemented in an Excel™ spreadsheet, assuming a time step of 10 s. To solve the problem, the time evolution of the total flux ($Jv$) and of the permeate stream concentration ($c_i^P$) is required; alternatively, the time evolution of the feed side concentration ($c_i^{FS}$) and the observed rejection ($R_{obs,i}$) can be used.

When NF is operated at an average constant flux value (as in STEP-mode), the corresponding observed rejections can be obtained by using the rejection vs. flux data reported in Fig. 4. Consequently, at any time $t$, the volume and the mass of the solute $i$ in the feed side can be calculated using Eqs. (10) and (11), respectively. In the case of operations at constant TMP values, the flux data as a function of VCF (as shown in Fig. 3a) can be used. As illustrated in the Figure inserted in Table 3, at any time $t$, the corresponding value of $VCF$ can be calculated from the mass balances of the previous step: correspondingly, $Jv$ can be obtained from the data in Fig. 3a) and the observed rejections can be

**Table 3**
Equations for simulating NF and DF operations (reference to Fig. 2).

total mass balance

$$\frac{dV^{FS}}{dt} = -J_v(t) \times A_m + Q_W(t) \quad (10)$$

mass balance for the *i-th* component

$$\frac{dm_i^{FS}}{dt} = -c_i^P(t) \times J_v(t) \times A_m = -c_i^{FS}(t) \times (1 - R_{obs,i}(t)) \times J_v(t) \times A_m \quad (11)$$

in which $c_i^{FS}(t) = \frac{m_i^{FS}(t)}{V^{FS}(t)}$

boundary conditions

$$V^{FS}(0) = V_0^{FS}$$
$$m_i^{FS}(0) = c_{i,0}^{FS} \times V_0^{FS}$$

in NF concentration mode: $Q_W(t) = 0$

in DF at constant volume: $Q_W(t) = Q_P(t) = J_v(t) \times A_m$

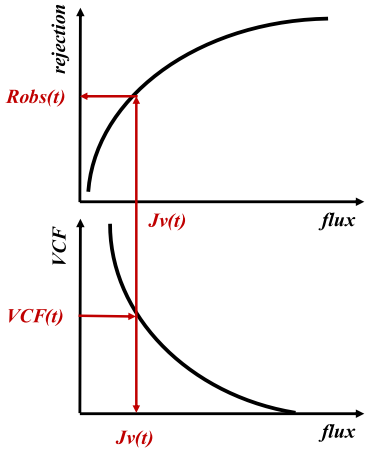


obtained from the data in Fig. 4, and then the integration process can be continued.

The same procedure can be followed to model NF in DF mode, which was performed at constant average flux; in this case, since the membrane is used at the same conditions of temperature, pH and velocity, the rejection vs. flux curves (Fig. 4) were used.

It is important to emphasize that in this case the term "semi-empirical model" is much more appropriate than "model" because the membrane performance data used are those obtained under specific operating conditions and should only be used to simulate performances of a DK membrane operating at the corresponding values.

All the results obtained by the simulations are plotted as "lines" in Figs. 5–8: the evidence of a very good quality of both the semi-empirical model and the simulation technique can be widely appreciated, both in the case of the artificial solution and of the real solution.

For the artificial solution, regarding the simulations of the NF in concentration mode (Fig. 5), the semi-empirical model obviously reproduces the experimental data, since the rejection vs. flux data were obtained in the same range of concentrations, temperature, pH and superficial velocity as the experiments. The largest discrepancy is observed for lactose loss (Fig. 5d), where the model appears to be conservative: in STEP-mode at VCF=3.77 the lactose loss is predicted to be 0.86% against a measured value of 0.80%. These differences are very insignificant, and in any case the lactose loss is always less than 1%.

The most interesting results are obtained in the DF simulation of the artificial solution, both for the "as it is" (Fig. 6) and after NF at VCF=2.12 (Fig. 7 and S4 of the Supplementary Information). In those cases, where the lactic acid concentration varied in the range from 4.4 to 0.8 g/dm$^3$ (as it can be observed in Fig. 6a)), the predicted lines are superimposed on the experimental data. This means that, although one would have expected an effect of the lactic acid concentration on its rejection, it was not evident in this case. The simulations carried out neglecting the concentration effect are in perfect agreement with the experimental results. It is therefore possible to extend the validity range of the membrane performances of Fig. 4, at least in the whole range studied, from 0.8 to 8 g/dm$^3$ of lactic acid. Any extrapolation outside this range must be done very carefully.

For the real solution, the prediction quality of the semi-empirical model is equally good, but with a slight increase in the discrepancy with the experimental data. However, it should be taken into account that this is a complex solution with the presence of divalent electrolytes, which can have an effect on the lactic acid rejection, since they are involved in the determination of the membrane charge, and also on the lactose rejection. In fact, a careful look at the results in Fig. 8 shows that the specification of LA/LT=0.03 g/g is experimentally achieved by operating at VDF=0.92; correspondingly, the model predicted lactic acid rejection is slightly overestimated (value of 81.6% compared to 79.7% experimental), which implies a slight underestimation of lactic acid rejection compared to experimental values. The effects, although modest, are also detectable in lactose loss, which is slightly underestimated by the model (value of 1.16% compared to 1.31% measured experimentally). Although, as with the artificial solution, these are very small numbers, a slight decrease in lactose rejection can be detected in the real solution, most likely due to a greater role of salting-out phenomena.

### 5.1. *Preliminary process analysis and discussion*

After demonstrating the validity of the semi-empirical model in predicting the performance of the DK membrane with an artificial solution and with a real solution, especially in predicting the LA/LT parameter, a preliminary process analysis was performed to study the efficiency of the integrated NF+DF process and to investigate the effect of some operating conditions.

The simulation was carried out assuming the artificial solution (Table 1) as the feed of the NF unit, NF and DF operating under the same conditions maintained during the experiments (50 °C, pH 4, DK membranes arranged in a 34-mil-feed-spacer spiral wound module at 0.36 m/s superficial velocity). The parameters investigated are: i) the behavior of the VDF in the DF step, ii) the final concentration of lactose achievable in the DF step, iii) the behavior of the TMP in the NF step, and iv) the specific area required in the NF step. All the parameters are reported as a

function of the VCF in the NF step.

The TMP in the NF step is estimated as reported in Eq. (12), in which the osmotic pressure difference is calculated at the bulk conditions, by neglecting the contributions of lactose and lactic acid in the permeate side; the contribution of salts was also neglected, since low rejections were measured for NaCl. Such an osmotic pressure calculation can be considered conservative in that it tends to overestimate the TMP required.

$$TMP = \Delta\pi + \frac{< J_v >}{L_{p,w}};\ \ \Delta\pi \simeq \pi_{LT}^{FS} + \pi_{LA}^{FS} \tag{12}$$

The specific area is defined as the membrane area (in $m^2$) required to process 1 $m^3$ of feed per hour in the NF step, as reported in Equation (13):

$$\text{specific area} = \frac{A_m}{V^{FS}/\Delta t} = \frac{VCF - 1}{VCF} \times \frac{1}{< J_v >} \tag{13}$$

where $< J_v >$ is the average flux obtained in the NF step.

The main results are reported in Figs. 9 and 10. In Fig. 9, the performances of the DF step have been simulated at an average flux of 9 $dm^3/(hm^2)$, while for the NF step the cases of average fluxes from 8 to 30 $dm^3/(hm^2)$ have been compared with the case of constant TMP at 20 bar; two specifications have been studied corresponding to LA/LT values of 0.04 and 0.03 g/g. The case of TMP=20 bar was also accounted as comparison with the operative conditions kept with similar membranes by other authors [8,19,21], cited as reference along this work.

Apparently, due to the very high lactose rejection, lactose permeation is strongly inhibited and the lactose concentration obtained in the DF retentate depends mainly on the VCF. Remarkably, the final lactose concentration of 120 $g/dm^3$ can be obtained with different combinations of VCF and VDF, depending on the desired LA/LT ratio and on the average flux set for the NF step. The target of LA/LT=0.03 g/g can be achieved by integrating the NF step, operating at VCF=4 and 8 $dm^3/(hm^2)$ with the DF step operating at VDF=0.52 and 9 $dm^3/(hm^2)$. Conversely, the same objective can be achieved by integrating the NF step, operating at VCF=4 and TMP=20 bar with the DF step operating at VDF=0.94 and 9 $dm^3/(hm^2)$.

The first case is clearly more favorable: it reduces the water consumption by 50% with respect to the second case; in addition, the maximum TMP required in the NF step is less than 20 bar. In fact, as can be seen in Fig. 10a), the TMP in the NF step operating at 8 $dm^3/(hm^2)$ should be regulated in the range from 4.5 to 12.5 bar; correspondingly

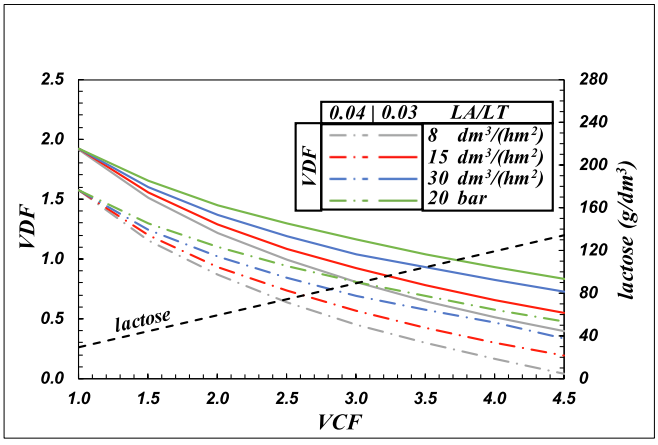


**Fig. 9.** Performance of the integrated NF+DF process calculated for the artificial solution: VDF and lactose concentration in the final retentate of the DF step are reported along the VCF in the NF step. Simulations performed at constant average fluxes and at TMP=20 bar in the NF step, with an average flux of 9 $dm^3/(hm^2)$ in the DF step. LA/LT=0.04 g/g (solid lines), LA/LT=0.03 g/g (dashed lines).

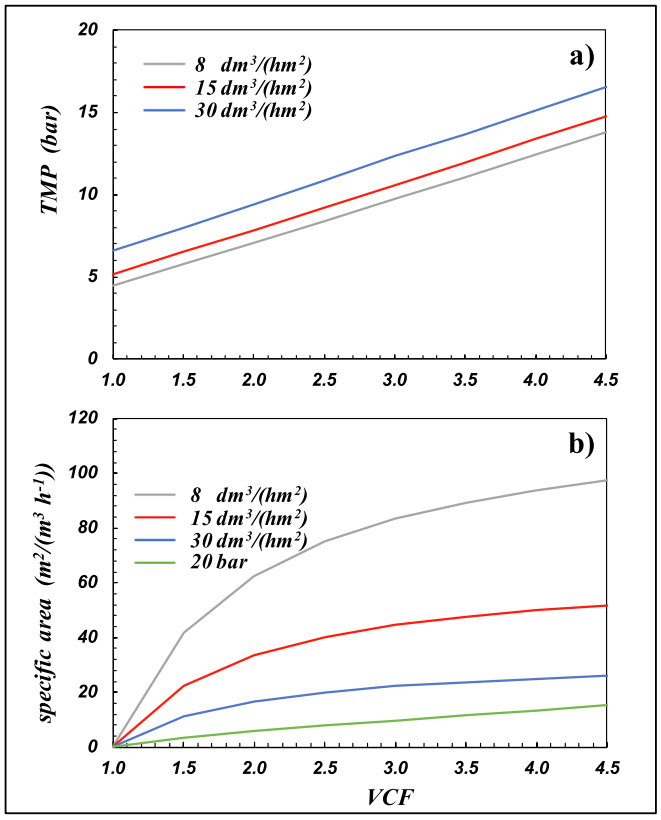


**Fig. 10.** Performance of the NF step before DF, calculated for the artificial solution: evolution a) of the TMP and b) of the specific area along the VCF. Simulations are reported at constant average fluxes and at TMP=20 bar.

the DF has been calculated to operate at almost 13 bar to ensure 9 $dm^3/(hm^2)$. It should be noted that there is a very good agreement with the TMP values that have been experimentally adjusted to obtain the results shown in Figs. 7 and 8.

Finally, by comparing Fig. 10a) with Fig. 10b), it is possible to observe that, by increasing the average flux from 8 to 15 $dm^3/(hm^2)$, there is a remarkable reduction of the specific area from 94 to 50 $m^2/(m^3h^{-1})$, setting the same targets of LA/LT=0.03 g/g and 120 $g/dm^3$ lactose. This advantage is also supported by a very low increase both of the TMP in the NF step (13 bar) and of the VDF required in the DF step (close to 0.66).

It is clear, therefore, that the main design quantities can be identified in the VCF of the NF stage and in the value of the average fluxes to be maintained in the NF and DF stages, which seem to be constrained in the range 8–30 $dm^3/(hm^2)$. The premises exist for a detailed process analysis which could also give an exhaustive overview of the energy and water consumption.

## 6. Conclusions

This work has demonstrated the feasibility of lactose recovery from pretreated acid whey by NF.

First, the flowsheet of a complete process for the recovery of products from raw acid whey has been presented: after the pretreatments necessary for the good operation of the UF unit, designed for the recovery of proteins, a decalcification unit followed by a NF step has been considered to ensure the softening, demineralization and lactic acid removal required to obtain the lactose quality demanded by the market.

Essentially, the overall process comprises the majority of the operations conventionally employed for lactose recovery from sweet whey and largely aligns with the processes successfully proposed by other authors for the decalcification and deacidification of acid whey. The

differences lie in the decalcification method and in the position of the calcium removal step in the overall flow sheet.

Sweet whey is typically softened by ion exchange resins, which would be more difficult to use in the case of acid whey, both because of the higher calcium content and the presence of lactic acid. Lactic acid would be removed by the resins, requiring more effort for their regeneration and preventing any subsequent recovery of lactic acid. The integration of an ED step with the NF stage has been proposed to obtain demineralized and deacidified acid whey powders; in such cases the residual streams containing electrolytes and lactate are considered as waste.

This work proposes the removal of calcium by precipitation prior to the lactose concentration and deacidification step, which is operated by an integrated NF+DF process. This avoids the ED unit and allows for a further recovery of lactic acid. From an economic standpoint, it is anticipated that the cost of calcium precipitation can be compensated for by avoiding the expense of the ED unit, by the operational benefits of using the same NF equipment with the same modules to perform NF+DF, and finally, by the additional revenue generated by the recovered lactic acid.

Based on the literature, the performance of each step was evaluated to estimate the characteristics of the input to the NF unit.

In general, this work represents the proof of concept of the feasibility of the step dedicated to the recovery and purification of lactose. The key points are the following.

a) The feasibility of lactose recovery after the decalcification step was first demonstrated by an experimental campaign performed with an artificial solution, containing lactose, lactic acid and sodium chloride. The NF+DF opportunity was finally tested with a real solution. It was shown that the maximum lactic acid removal, close to 87.6%, was obtained by operating with a NF step (at VCF=3.52) followed by a NF step operating in DF at constant volume (at VDF=1.81), ensuring a lactic acid/lactose ratio of 0.018 g/g and an overall lactose purity and yield of 93.6% and 98.2%, respectively.
   Transmembrane pressure was identified as the key parameter for the success of the process: the better separation efficiency was obtained at low pressure values to ensure average fluxes in the range of 8 to 10 $dm^3/(hm^2)$.
   The most interesting conclusion is that, contrary to the use of other membranes of the same type, as done by other authors, the DK membrane turns out to be the best compromise to simultaneously achieve a very high lactose rejection (not less than 98.5–99%), in order to keep the lactose yield high, and a low lactic acid rejection (not more than 20–30%), in order to obtain high degrees of deacidification.

b) The artificial solution was found to be a good approximation of the real solution. The semi-empirical model developed to describe the observed rejection of lactose and lactic acid is found to be valid for simulating the performance of a spiral module with a DK membrane, operating at pH 4, 50 °C, with a superficial velocity of 0.36 m/s. The model was also found to be valid for predicting lactic acid removal and lactose yield in the real solution and, more importantly, very useful in explaining the modest differences between real and artificial solutions. For a comprehensive study of the problem, experiments can then be carried out with the artificial solution, which is easier to handle, in order to perform a detailed study of the role of operational variables. Conversely, the semi-empirical model can be used to run simulations to address the experiments for the final scale-up.

c) The proof of concept was completed by a preliminary process analysis of the integrated NF+DF configuration, which proved that the most important design quantities are the VCF, which determines the final lactose concentration, and the average fluxes in the NF step, which could be constrained in the range of 8 to 30 $dm^3/(hm^2)$. The premises for a detailed process development are given.

## CRediT authorship contribution statement

**Marco Roselli:** Investigation, Data curation, Conceptualization. **Riccardo Onesti:** Writing – original draft, Methodology, Data curation. **Cristiana Boi:** Writing – review & editing, Supervision, Funding acquisition. **Serena Bandini:** Writing – original draft, Supervision, Project administration, Methodology, Funding acquisition, Formal analysis, Conceptualization.

## Declaration of competing interest

The authors declare that they have no known competing financial interests or personal relationships that could have appeared to influence the work reported in this paper.

## Acknowledgements

The authors acknowledge financial support from PNRR MUR project ECS_00000033_ECOSISTER and from the University of Bologna. Marco Roselli acknowledges the PON scholarship funded with FSE REACT-EU resources.

Reire-srl is gratefully acknowledged for providing the ultrafiltered whey powder.

## Appendix A. Supplementary data

Supplementary data to this article can be found online at https://doi.org/10.1016/j.seppur.2024.128303.

## References

[1] V.A. Kravtsov, I.K. Kulikova, G.S. Anisimov, I.A. Evdokimov, A.G. Khramtsov, Variety of dairy ultrafiltration permeates and their purification in lactose production, IOP Conf. Ser.: Earth Environ. Sci. 677 (2021) 032001, https://doi.org/10.1088/1755-1315/677/3/032001.
[2] D. Buchanan, W. Martindale, E. Romeih, E. Hebishy, Recent advances in whey processing and valorisation: Technological and environmental perspectives, Int. J. Dairy Techol. 76 (2023) 291–312, https://doi.org/10.1111/1471-0307.12935.
[3] N. Kaur, P. Sharma, S. Jaimni, B.A. Kehinde, S. Kaur, Recent developments in purification techniques and industrial applications for whey valorization: A review, Chem. Eng. Commun. 207 (2020) 123–138, https://doi.org/10.1080/00986445.2019.1573169.
[4] H.N. Blais, K. Schroën, J.T. Tobin, A review of multistage membrane filtration approaches for enhanced efficiency during concentration and fractionation of milk and whey, Int. J. Dairy Technol. 75 (2022) 749–760, https://doi.org/10.1111/1471-0307.12884.
[5] Applexion, Novasep membrane filtration, (2024). Retrieved from https://applexion.com. Accessed February 5, 2024.
[6] E.N. Nielsen, A. Merkel, S.R. Yazdi, L. Ahrné, The effect of acid whey composition on the removal of calcium and lactate during electrodialysis, Int. Dairy J. 117 (2021) 104985, https://doi.org/10.1016/j.idairyj.2021.104985.
[7] G.Q. Chen, F.I.I. Eschbach, M. Weeks, S.L. Gras, S.E. Kentish, Removal of lactic acid from acid whey using electrodialysis, Sep. Purif. Technol. 158 (2016) 230–237, https://doi.org/10.1016/j.seppur.2015.12.016.
[8] S. Talebi, F. Suarez, G.Q. Chen, X. Chen, K. Bathurst, S.E. Kentish, Pilot Study on the Removal of Lactic Acid and Minerals from Acid Whey Using Membrane Technology, ACS Sustainable Chem. Eng. 8 (2020) 2742–2752, https://doi.org/10.1021/acssuschemeng.9b06561.
[9] A. Merkel, D. Voropaeva, M. Ondrušek, The impact of integrated nanofiltration and electrodialytic processes on the chemical composition of sweet and acid whey streams, J. Food Eng. 298 (2021) 110500, https://doi.org/10.1016/j.jfoodeng.2021.110500.
[10] P. Menchik, T. Zuber, A. Zuber, C.I. Moraru, Short communication: Composition of coproduct streams from dairy processing: Acid whey and milk permeate, J. Dairy Sci. 102 (2019) 3978–3984, https://doi.org/10.3168/jds.2018-15951.
[11] M. Bédas, G. Tanguy, A. Dolivet, S. Méjean, F. Gaucheron, G. Garric, G. Senard, R. Jeantet, P. Schuck, Nanofiltration of lactic acid whey prior to spray drying: Scaling up to a semi-industrial scale, LWT Food Sci. Technol. 79 (2017) 355–360, https://doi.org/10.1016/j.lwt.2017.01.061.
[12] J. Chandrapala, R. Wijayasinghe, T. Vasiljevic, Lactose crystallization as affected by presence of lactic acid and calcium in model lactose systems, J. Food Eng. 178 (2016) 181–189, https://doi.org/10.1016/j.jfoodeng.2016.01.019.

[13] R. Wijayasinghe, T. Vasiljevic, J. Chandrapala, Lactose behaviour in the presence of lactic acid and calcium, J. Dairy Res. 83 (2016) 395–401, https://doi.org/10.1017/S0022029916000315.
[14] J. Chandrapala, T. Vasiljevic, Properties of spray dried lactose powders influenced by presence of lactic acid and calcium, J. Food Eng. 198 (2017) 63–71, https://doi.org/10.1016/j.jfoodeng.2016.11.017.
[15] J. Chandrapala, T. Vasiljevic, Feasibility of spray drying concentrated acid whey after nanofiltration, Food Bioprocess. Technol. 11 (2018) 1505–1515, https://doi.org/10.1007/s11947-018-2118-1.
[16] C. Darmali, S. Mansouri, N. Yazdanpanah, Z.K. Nagy, M.W. Woo, Continuous lactose recovery from acid whey by mixed suspension mixed product removal (MSMPR) crystallizer in the presence of impurities, Chem. Eng. Process. – Process Intesif. 180 (2022) 108752, https://doi.org/10.1016/j.cep.2021.108752.
[17] M.A. Theoleyre, F. Gula, Purification of food streams by combining ion exchange and membranes technologies: application of decalcification in the whey industry, Int. Conf. Eng. Food (2004).
[18] A. Román, J. Wang, J. Csanádi, C. Hodúr, G. Vatai, Partial demineralization and concentration of acid whey by nanofiltration combined with diafiltration, Desalination 241 (2009) 288–295, https://doi.org/10.1016/j.desal.2007.12.054.
[19] J. Chandrapala, M.C. Duke, S.R. Gray, M. Weeks, M. Palmer, T. Vasiljevic, Nanofiltration and nanodiafiltration of acid whey as a function of pH and temperature, Sep. Purif. Technol. 160 (2016) 18–27, https://doi.org/10.1016/j.seppur.2015.12.046.
[20] J. Chandrapala, M.C. Duke, S.R. Gray, M. Weeks, M. Palmer, T. Vasiljevic, Strategies for maximizing removal of lactic acid from acid whey – Addressing the un-processability issue, Sep. Purif. Technol. 172 (2017) 489–497, https://doi.org/10.1016/j.seppur.2016.09.004.
[21] J. Chandrapala, G.Q. Chen, K. Kezia, E.G. Bowman, T. Vasiljevic, S.E. Kentish, Removal of lactate from acid whey using nanofiltration, J. Food Eng. 177 (2016) 59–64, https://doi.org/10.1016/j.jfoodeng.2015.12.019.
[22] G. Dufton, S. Mikhaylin, S. Gaaloul, L. Bazinet, How electrodialysis configuration influences acid whey deacidification and membrane scaling, J. Dairy Sci. 101 (2018) 7833–7850, https://doi.org/10.3168/jds.2018-14639.
[23] M. Belleville, J. Sanchez-Marcano, G. Bargeman, M. Timmer, Nanofiltration in the Food Industry, in: Nanofiltration, 2nd ed.,, Wiley, 2021, pp. 499–542.
[24] E.N. Nielsen, L.H. Skibsted, S.R. Yazdi, A. Merkel, L.M. Ahrné, Improving electrodialysis separation efficiency of minerals from acid whey by nano-filtration pre-processing, Int. J. Dairy Technol. 75 (2022) 820–830, https://doi.org/10.1111/1471-0307.12893.
[25] R.R. de Souza, R. Bergamasco, S.C. da Costa, X. Feng, S.H.B. Faria, M.L. Gimenes, Recovery and purification of lactose from whey, Chem. Eng. Process. 49 (2010) 1137–1143, https://doi.org/10.1016/j.cep.2010.08.015.
[26] C. Casado-Coterillo, P. Díaz-Guridi, J.A. Otero, R. Ibáñez, Modeling of lactic acid rejection from lactose in acidified cheese whey by nanofiltration, J. Dairy Sci. 106 (2023) 4533–4544, https://doi.org/10.3168/jds.2022-22502.
[27] H. Ye, J. Lei, Y. Zhang, H. Li, G. Li, Z. Cao, L. Xie, Investigation of microfiltration for pretreatment of whey concentration, Desalin. Water Treat. 34 (2011) 173–178, https://doi.org/10.5004/dwt.2011.2914.
[28] F. Ostertag, E. Krolitzki, S. Berensmeier, J. Hinrichs, Protein valorisation from acid whey – Screening of various micro- and ultrafiltration membranes concerning the filtration performance, Int. Dairy J. 146 (2023) 105745, https://doi.org/10.1016/j.idairyj.2023.105745.
[29] C. Baldasso, W.P. Silvestre, N. Silveira, A.P. Vanin, N.S.M. Cardozo, I.C. Tessaro, Ultrafiltration and diafiltration modeling for improved whey protein purification, Sep. Sci. Technol. 57 (2022) 1926–1935, https://doi.org/10.1080/01496395.2021.2021424.
[30] A.G. Ortiz Quezada, A. Castilla Asaf, G.L. Sacks, Optimization of conditions for Greek style yogurt acid whey demineralization and its effects on filterability, Int. Dairy J. 123 (2021) 105163, https://doi.org/10.1016/j.idairyj.2021.105163.
[31] A. Kumar, A. Thakur, P.S. Panesar, Lactic acid and its separation and purification techniques: a review, Rev. Environ. Sci. Biotechnol. 18 (2019) 823–853, https://doi.org/10.1007/s11157-019-09517-w.
[32] R. Alves De Oliveira, M. Alexandri, A. Komesu, J. Venus, C.E. Vaz Rossell, R. Maciel Filho, Current Advances in Separation and Purification of Second-Generation Lactic Acid, Separat. Purif. Rev. 49 (2020) 159–175, https://doi.org/10.1080/15422119.2019.1590412.
[33] R.C. Weast, D.R. Lide, CRC Handbook of Chemistry and Physics, 70th edition, CRC Press, 1989.
[34] Veolia Water Technologies & Solutions, Veolia DK Series Fact sheet, (2024). Retrieved from https://www.lenntech.com/Data-sheets/Veolia-DK-Seires-EN-L.pdf. Accessed January 10, 2024.
[35] S. Bandini, V. Morelli, Effect of temperature, pH and composition on nanofiltration of mono/disaccharides: Experiments and modeling assessment, J. Membr. Sci. 533 (2017) 57–74, https://doi.org/10.1016/j.memsci.2017.03.021.
[36] J.M.B. Domingos, G.A. Martinez, E. Morselli, S. Bandini, L. Bertin, Reverse osmosis and nanofiltration opportunities to concentrate multicomponent mixtures of volatile fatty acids, Separ. Purif. Technol. 290 (2022) 120840, https://doi.org/10.1016/j.seppur.2022.120840.
[37] S. Bandini, J. Drei, D. Vezzani, The role of pH and concentration on the ion rejection in polyamide nanofiltration membranes, J. Membr. Sci. 264 (2005) 65–74, https://doi.org/10.1016/j.memsci.2005.03.054.
[38] W.R. Bowen, J.S. Welfoot, Modelling the performance of membrane nano#ltration—critical assessment and model development_, Chem. Eng. Sci. (2002).
[39] D.L. Oatley, L. Llenas, R. Pérez, P.M. Williams, X. Martínez-Lladó, M. Rovira, Review of the dielectric properties of nanofiltration membranes and verification of the single oriented layer approximation, Adv. Colloid and Interface Sci. 173 (2012) 1–11, https://doi.org/10.1016/j.cis.2012.02.001.
[40] D.L. Oatley-Radcliffe, S.R. Williams, M.S. Barrow, P.M. Williams, Critical appraisal of current nanofiltration modelling strategies for seawater desalination and further insights on dielectric exclusion, Desalination 343 (2014) 154–161, https://doi.org/10.1016/j.desal.2013.10.001.
[41] S. Bandini, V. Morelli, Mass transfer in,, spiral wound modules: Experimental study in dextrose-water nanofiltration, Separ. Purif. Technol. 199 (2018) (1812) 84–96, https://doi.org/10.1016/j.seppur.2018.01.044.
[42] M.I. González, S. Alvarez, F.A. Riera, R. Álvarez, Lactic acid recovery from whey ultrafiltrate fermentation broths and artificial solutions by nanofiltration, Desalination 228 (2008) 84–96, https://doi.org/10.1016/j.desal.2007.08.009.
[43] Y. Zhu, S. Galier, H. Roux-de Balmann, Description of the variation of retention versus pH in nanofiltration of organic acids, J. Membr. Sci. 637 (2021) 119588, https://doi.org/10.1016/j.memsci.2021.119588.
[44] G. Rice, A.R. Barber, A.J. O'Connor, G.W. Stevens, S.E. Kentish, Rejection of dairy salts by a nanofiltration membrane, Separat. Purif. Technol. 79 (2011) 92–102, https://doi.org/10.1016/j.seppur.2011.03.022.
[45] C. Umpuch, S. Galier, S. Kanchanatawee, H.R. Balmann, Nanofiltration as a purification step in production process of organic acids: Selectivity improvement by addition of an inorganic salt, Process Biochem. 45 (2010) 1763–1768, https://doi.org/10.1016/j.procbio.2010.01.015.
[46] B. Cuartas-Uribe, M.I. Alcaina-Miranda, E. Soriano-Costa, J.A. Mendoza-Roca, M. I. Iborra-Clar, J. Lora-García, A study of the separation of lactose from whey ultrafiltration permeate using nanofiltration, Desalination 241 (2009) 244–255, https://doi.org/10.1016/j.desal.2007.11.086.
[47] S. Bandini, C. Boi, Transport phenomena in reverse osmosis/nanofiltration membranes. In Current Trends and Future Developments on (Bio-) Membranes, Elsevier: Amsterdam, The Netherlands, 2021; pp. 49–90.
[48] C. Mazzoni, L. Bruni, S. Bandini, Nanofiltration: Role of the Electrolyte and pH on Desal DK Performances, Ind. Eng. Chem. Res. 46 (2007) 2254–2262, https://doi.org/10.1021/ie0609741.
[49] W.H. Press, S.A. Teukolsky, W.T. Vetterling, B.P. Flannery (Eds.), Numerical Recipes: the Art of Scientific Computing, 3rd ed, Cambridge University Press, Cambridge, UK, New York, 2007.